Bone Water Concentration as a New Metric for Cortical Bone Quality

H. Salighehi Rad[1], J. Love[1], J. F. Magland[1], M. F. Leonard[2], and F. W. Wehrli[1]
[1]Laboratory for Structural NMR Imaging, Department of Radiology, University of Pennsylvania Health System, Philadelphia, PA, United States, [2]Nephrology, Children's Hospital of Philadelphia, Philadelphia, PA, United States

Introduction

Age-related increase in cortical bone porosity is a major cause of the impaired strength of osteoporotic cortical bone **[1,2]**. While increased porosity results in decreased areal or volumetric bone mineral density (BMD), the pores are below the resolution limit achievable in vivo. Therefore, an increase in pore volume in the presence of normally mineralized bone cannot be distinguished from the situation wherein the pore volume is unaltered but the bone is under-mineralized as, for example, in osteomalacia. On the other hand, there is no broad agreement that the intrinsic mechanical properties of osteoporotic bone are different from those of normal bone. Rather, the impaired strength of osteoporotic cortical bone is a consequence of increased pore volume fraction **[2]**. The spaces of the haversian and lacuno-canalicular system making up the total pore volume are fluid-filled, essentially consisting of water while another fraction is collagen bound. Even though not equivalent to porosity, knowledge of bone water concentration (BWC) would provide a measure of the pore volume. Here we introduce the BWC, measured noninvasively by solid-state proton imaging **[3,4,5]** of cortical bone **[6,7]**, as a new metric of cortical bone quality, and then compare it with other metrics of cortical bone quality, including areal- and volumetric BMD in healthy men and women covering a wide age range to establish a normal baseline of cortical BW.

Methods

Recruitment, inclusion and exclusion criteria: Healthy men and women covering the age range from 26 to 80 years (N=34) with body mass index (BMI) < 30 kg/m^2 and dual energy X-ray absorptiometry (DXA) BMD z-scores at both spine and hip meeting the criteria $-2 \le Z \le 2$ were scanned. Subjects with medical histories that indicate disorders (e.g. malabsorption syndromes, renal or hepatic disease), surgery, or treatments compromising bone mineral homeostasis, were excluded.

Image acquisition and processing: A 3D hybrid radial UTE (3DHRUTE) sequence with selective excitation half-sinc pulses (slab thickness=5cm, flip-angle=23˚) was used to acquire twenty axial slices of the left tibial mid-shaft using an 8-channel Tx/Rx knee coil on a 3T Siemens Tim Trio scanner (Erlangen, Germany). The FOV of 180×180×90mm^3 was centered at 38% of the tibia length (site of maximum cortical thickness) as measured from the medial malleolus, 500 radial projections of 256 readout points (dwell time = 6μsec, $BW_{\text{read-out}}$ = 650 Hz/pixel) were acquired using a TR of 20msec, yielding a voxel size of 0.38×0.38×4.5mm^3 in 6.6mins. Radial readout with ramp sampling requires regridding which is accurately performed using a gradient mapping calibration technique. Image analysis and reconstruction is performed using MATLAB 7.5 (The MathWorks). No soft-tissue suppression was used to avoid systematic errors from partial suppression of the BW signal.

BWC quantification: Fig. 1 illustrates different steps of image analysis and quantification of BWC as follows: 1) regridding reconstruction of the two UTE images and correction for coil shading using a 3D coil profile, 2) segmentation of the cortical bone region from the soft tissue and fatty marrow by delineating periosteal and endosteal boundaries using a specialized region growing segmentation program, 3) slice-by-slice calculation of T_1-maps and BWC-maps for each pixel within the segmented bone region. BWC is calculated by comparing the intensities of bone pixels with that of external references of known parameters (thin tube phantoms filled with 20% H_2O in D_2O doped with 27mM $MnCl_2$ yielding T_1~15msec and T_2^*~320μsec) attached to the subject's leg and centered at the site of 38% of the tibia length **[7]**.

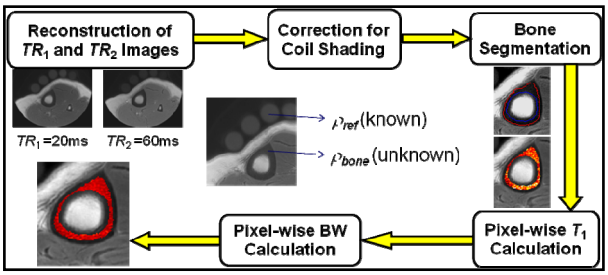

Figure 1: Image analysis and BWC quantification flow diagram.

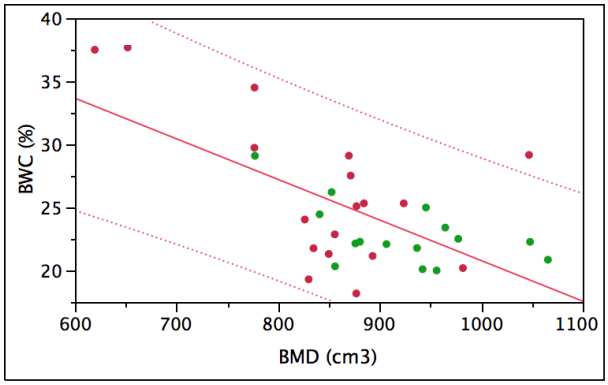

Figure 2: BWC (%) vs. volumetric-BMD (mg/cm^3) in 38%Tibia (R = -0.64, p < 0.0001, N=34, • M, • F).

Results and Conclusions:

Fig. 2 shows BWC versus volumetric BMD in 34 healthy men and women (as measured by peripheral quantitative CT (pQCT) at the 38% site of the left tibial midshaft) showing a negative correlation (R = -0.64, p < 0.0001). Similar negative correlations were also found between BWC and areal BMD (R = -0.55, p = 0.0008) and R = -0.56, p = 0.0005) for measurements at the hip and the spine, respectively. BWC increased with age (R = 0.50), more so in women than in men, but the increase was highly nonlinear, increasing sharply after age 50, in particular in women. A correlation matrix for the various parameters is given in Table 1.

In conclusion, our results suggest BWC to be reciprocally related to BMD and increasing in both genders with age, presumably as a result of increasing cortical porosity.

	BWC%	Hip_BMD (gr/cm^2)	Spine_BMD (gr/cm^2)	Tibia_BMD (gr/cm^3)
Hip_BMD (gr/cm^2)	-0.55 (p=0.0008)	--		
Spine_BMD (gr/cm^2)	-0.56 (p=0.0005)	0.80 (p<0.0001)	--	
Tibia_BMD (gr/cm^3)	-0.64 (p<0.0001)	0.54 (p=0.001)	0.41 (p=0.016)	--
Age (N=34)	0.50 (p<0.003)	-0.11 (p=0.53)	-0.07 (p=0.68)	-0.49 (p=0.0034)
Age_Female (N=19)	0.58 (p=0.0094)	-0.10 (p=0.67)	-0.12 (p=0.61)	0.57 (p=0.14)
Age_Male (N=15)	0.41 (p=0.13)	-0.04 (p=0.90)	0.07 (p=0.81)	0.37 (p=0.17)

Table 1: Correlations (R) between BWC, areal BMD of hip and spine, volumetric BMD at 38% tibia and age (N=34).

References: **[1]** Seeman E *et al.*, *NEJM* 354, 2250 (2006). **[2]** Bousson V *et al*, *JBMR* 19, 794 (2004). **[3]** Robson MD *et al.*, *JCAT* 27, 825 (2003). **[4]** Du J *et al, MRM,* 62, 527 (2009). **[5]** Bydder GM *et al., Skel Radiology,* 38, 201 (2009). **[6]** Robson *et al.*, *NMR Biomed* 19,765 (2006). **[7]** Techawiboonwong A *et al.*, *Radiology* 248, 824 (2008).

Acknowledgements: ***NIH grant RO1 AR50068***